Heliyon 10 (2024) e35552

Contents lists available at ScienceDirect

Heliyon

journal homepage: www.cell.com/heliyon

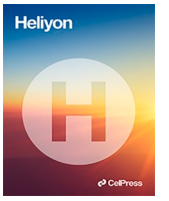

Research article

Investigation of mechanical and physico-chemical properties of new natural fiber extracted from *Bassia indica* plant for reinforcement of lightweight bio-composites

Djamila Kouidri [a,b], Mansour Rokbi [a], Zine Elabidine Rahmouni [a,c], Younes Kherbiche [a], Samira Bouchareb [a,b], Sanjay Mavinkere Rangappa [d,*], Suchart Siengchin [d]

[a] *Department of mechanical Engineering, Faculty of technology, University of M'sila, University pole, Bordj Bou Arreridj road, M'Sila 28000 Algeria*
[b] *Laboratoire de Matériaux et Mécanique des Structures (LMMS). Université de M'sila, Algeria*
[c] *Department of Civil Engineering, Faculty of technology, University of M'sila, M'sila, Algeria*
[d] *Natural Composites Research Group Lab, Department of Materials and Production Engineering, The Sirindhorn International Thai-German School of Engineering (TGGS), King Mongkut's University of Technology North Bangkok (KMUTNB), Bangkok -10800, Thailand*

ARTICLE INFO

Keywords:
Bassia indica
Cellulose fibers
ATR-FTIR
Thermal analysis
Weibull statistics
XRD
Mechanical properties

ABSTRACT

In this investigation, novel cellulose fibers were acquired from the *Bassia Indica* plant to serve as a reinforcement source in composite materials. The morphological characteristics were studied using Scanning Electron Microscopy (SEM). The surface chemistry, crystallinity, and functional groups of *Bassia Indica* fibers were analyzed using X-ray Diffraction (XRD), Energy Dispersive X-ray (EDX) spectroscopy, and Attenuated Total Reflectance-Fourier Transform Infrared spectroscopy (ATR-FTIR), which assess the crystal structure, elemental composition, and surface functional groups, respectively. The thermal behavior of *Bassia Indica* fibers were assessed through Thermogravimetric Analysis (TGA). Anatomical techniques demonstrated the abundant presence of fibroblasts in the fibers. The presence of lignocellulosic fiber (lignin, cellulose and hemicellulose) was confirmed through ATR-FTIR analysis. The analysis of physical properties unveiled a fiber density of 1.065 ± 0.025 g/cm^3 and a diameter of 145.58 ± 7.89 μm. The crystalline size of *Bassia Indica* fibers reached 2.23 nm, with a crystallinity index of 40.12 %, and an activation energy of 93.78 kJ/mol, TGA research revealed that *Bassia Indica* fibers are thermally stable up to 260.24 °C. Additionally, the fibers experienced maximum degradation at 321.23 °C. Weibull statistical analysis was performed using parameters 2 and 3 to calculate the observed dispersion in the experimental tensile results after analyzing the mechanical properties of the fibers possessing a tensile strength of 417.50 ± 7.08 MPa, Young's modulus of 17.46 ± 1.55 GPa, stress at failure of 1.17 ± 0.02 % and interfacial shear strength of 6.99 ± 1.10 MPa. The results were additionally compared to how they were stated in the relevant sources. *Bassia Indica* fibers can be considered a viable choice for reinforcing lightweight bio-composites.

* Corresponding author.
E-mail address: mavinkere.r.s@op.kmutnb.ac.th (S. Mavinkere Rangappa).

https://doi.org/10.1016/j.heliyon.2024.e35552
Received 21 January 2024; Received in revised form 31 July 2024; Accepted 31 July 2024
Available online 3 August 2024

1. Introduction

In recent years, growing environmental consciousness have motivated researchers, industries and scientists to develop innovative and eco-friendly materials. In other words, developing new products that are easily recyclable or biodegradable. Raw material selection is the initial step of a sustainable production chain [1,2]. The integration of natural fibers, as a strengthening element in polymers composites, has resulted in the development of a variety of products suitable for different industries including automobiles, aviation, marine, building materials, textiles and domestic applications. This is due to their advantageous properties compared to synthetic ones [3]. These features include low density and cost, biodegradability, ready availability in the environment, easily extractable, thermal insulation and no toxicity [4,5]. Moreover, natural fibers are recognized for their eco-friendliness, as they release minimal to no harmful gases into the environment [6], In addition, composites reinforced with natural fibers offer easy fabrication properties that are less hazardous compared to traditional composites [7,8].

The demand to replace synthetic fibers with natural cellulosic fibers is substantial. This increasing acceptance has compelled researchers to investigate new natural fibers with suitable properties. Conversely, the current production of natural fibers falls short of meeting industry needs [9,10]. Thousands of species of natural fibers are available in nature, but only a few of them have been used as reinforcing elements in composite materials. Despite the fact that natural fibers often contain cellulose, hemicellulose, pectin, lignin, wax and moisture, these composites cause less allergic responses and no serious discomfort in the human body is reported during their use [11]. Additionally, geological conditions for plant growth, nature and age of the plant, the part of the plant from which the fiber is extracted, the adopted extraction technique, all have a substantial impact on the final fiber quality [12]. Natural ligno-cellulosic fibers which has been derived from various plant parts such as root, stem, bark or leaf, are considered the most significant sources of cellulosic fibers [13]. Various techniques are adopted for fiber extraction. One of them involves immersing the plant parts in water (retting) [14], while others utilize mechanical or chemical processes [15,16]. These cost-effective methods significantly reduce amorphous components such as hemicellulose and lignin, resulting in improvements in the chemical composition, surface qualities, and then, good mechanical properties of the fibers were achieved [17]. Hence, the increasing demand for natural cellulosic fibers has prompted the search for new fibers with desired properties [18]. To develop a new category of environmentally friendly composite materials, a thorough understanding of fibers is crucial. Numerous studies have previously focused on commonly available and widely used fibers such as Jute (*Corchorus*), Cotton, Grass, Sisal (*Agave sisalana*), Ramie, Hemp (*Cannabis sativa*), Rice husk, Pineapple leaf fibers, Flax (*Linum usitatissimum*), Sugar cane, Kenaf (*Hibiscus cannabinus*) and Coir (*Cocos nucifera*). Furthermore, fibers obtained from specific plants in certain geographical regions and may not be easily accessible everywhere [19,20]. Researchers around the globe are presently exploring the possibilities presented by recently discovered natural cellulosic fibers, which originate from plants and trees abundant in local regions and renowned for their naturally high fiber content. Consequently, several natural fibers have been thoroughly examined for their suitability in creating robust composite structures [21]. Prithiviraj et al. [22] highlighted the significant

Fig. 1. Bassia Indica plant.

need for high-strength natural fiber composites in many areas, particularly in the automotive industry, to enhance fuel efficiency while preserving performance. Arthanarieswaran et al. [23] conducted a study on the white *Acacia leucophloea* plant's bark to explore its potential use as a capsule coating for improved swallowing and digestion. Bhunia, Anup Kumar et al. [24] investigated on new bio-fibers of *Cyperus Compactus (Cyperaceae)*. Their results revealed that it exhibit thermal stability at 227 °C and a kinetic energy of activation of 118.90 kJ/mol. Raouf Khaldoune, Rokbi [25] conducted a characterization of the *Centaurea melitensis* fibers. X-ray diffraction analysis revealed that the fiber crystals had a size of 16.92 nm. The authors proposed that improving fiber strength could be attained by enhancing the crystal structure and reducing the amorphous structure through chemical treatments. Selvaraj, Manivel et al. [26] explored a novel ligno-cellulosic fiber extracted from the bark of the *Ficus Carica* plant. The resulting fiber shows a density of 1.42 g/cm^3, with a measured tensile strength of 482 ± 6 MPa and an elongation at break ranging from 2.72 % to 4.91 %. According to the report by Bhunia, Anup Kumar et al. [27] the fiber obtained from the *Cyperus platystylis* plant demonstrated a higher crystalline index value of 41.12 %. Additionally, the suggested natural fiber exhibits a measured crystallite size of 2.28 nm. In their research, Belaadi, Ahmed et al. [28] characterized a novel natural fiber extracted from the *Yucca treculeana* L. leaf. Their results indicate that this proposed fiber exhibits excellent thermal stability at 293.5 °C, making it a favorable choice for developing polymer composites intended for high temperature applications. Gedik, Gorkem [29] conducted an investigation on fibers extracted from *Trachelospermum jasminoides (star jasmine)*, which exhibits a higher crystallinity index of 87.68 %, indicating their higher cellulose content and crystalline nature. Other recent studies have directed their investigation towards newly discovered natural fibers from *Purple bauhinia* [30], *Cissus vitiginea stem* [31] and *Derris scandens stem* [32].

The comprehensive literature study aids in comprehending the importance of natural fiber characterization. With the aim of creating environmentally friendly composites, a new cellulosic fiber has been extracted from the stems of *Bassia Indica* plants. *Bassia Indica* (BI) plants (commonly named *Kochia indica)*, belonging to the *Amaranthaceae* family, are small shrubs found to tropical and subtropical regions across various countries, ranging from the western Mediterranean to eastern Asia. These plants' leaves have a special therapeutic benefit and are also commonly used as ornaments. The stems are light and branching, brown to yellowish, with many spreading branches from the base and distant leaves (Fig. 1) [33,34].

To our knowledge, this is the first time that the *Bassia Indica* fiber has undergone a comprehensive characterization process. In this study, the examined fibers underwent a series of experiments, including morphological studies, assessments of surface properties, examinations of functional groups, analyses of mechanical properties, measurements of both density and diameter, examinations of crystalline properties, analyses of chemical composition and evaluations of activation energy and thermal stability properties. Experimental investigations encompassed Attenuated Total Reflectance Fourier Transform Infrared spectroscopy (ATR-FTIR), Thermogravimetric analysis (TGA), X-ray Diffraction (XRD) and scanning electron microscopy (SEM). Moreover, the outcomes of this study are compared with those of other recognized natural cellulosic fibers, utilizing the most trustworthy references found in the literature.

Fig. 2. Steps to obtain fiber: (a) BI plant, (b) water retting, (c) extracting BIFs.

2. Materials and methods

2.1. Raw material

A substantial quantity of *Bassia Indica* stems was collected in November from the Hodna region of M'sila, Algeria, the location-specific geocoordinates were 4° 32′ 49″ E, 35° 42′ 7″ N. *BI* stems are yellow or sometimes reddish in color, with a diameter of 0.3–0.9 cm, and a length of 0.4–1.8 m. *BI* plant is commonly found spreading on dry forest floors and waysides.

2.2. Fiber extraction

As shown in Fig. 2, the *BI* fibers (*BIF*s) were extracted from the *Bassia Indica* plant (Fig. 2a) by using a microbial degrading process. Following harvesting, *BI* stems were firstly separated from their branches and leaves. After that, they were cleaned of impurities using distilled water before being submerged in tap water inside a water basin (Fig. 2b), allowing microbial decomposition to occur over a period of 4 weeks at ambient temperature. This method promoted anaerobic bacterial activity, resulting in the decomposition of pectin and the cellular tissue around the bast fiber bundles. This process made fiber extraction easier by manual separation see (Fig. 2c). Finally, *BIF*s were washed repeatedly using distilled water and then dried in oven at 70 °C for 7 h. This approach not only resulted in water conservation through usual immersion period, like in the plants Syagrus Romanzoffiana [14] and Cyperus pangorei [35], which were immersed for up to 30 days, but also reduced extraction expenses. It proves to be more economical compared to the water retting technique, which demands significant quantities of purified water [36,37].

2.3. Morphological analysis

2.3.1. Anatomy of BI stem

The study of plant anatomy is an important technique for understanding plant structure. In this study, an anatomical analysis was conducted on a cross-section of the *Bassia Indica* (*BI*) stem. The transversal sections of *BI* stem thickness, ranging from 10 to 25 μm, were made using microtome. To enhance the visibility of structures, many *BI* stem sections were stained and affixed to glass slides. A mixture of Methylene blue was used for staining, ensuring clear and detailed images. Subsequently, the prepared slides were examined under a microscope (OPTIKA B-350). Many photographs were taken, and the best ones were selected for this study.

2.3.2. BIFs morphology

SEM images are instrumental in the analysis of surface morphology, porosity, surface roughness, cell wall structure, etc. This high-resolution imaging technique provides a detailed view of material surfaces and topography, following established protocols. Scanning Electron Microscope (TESCAN model VEGA3) to explore the surface morphology of *BI* fiber. The morphological study was conducted under high vacuum conditions, with an electron beam accelerating potential of 5 kV, following the application of a gold-palladium (Au–Pd) layer to the samples. This coating ensured high-resolution imaging and prevented electron beam charging effects during the examination. Micrographs were captured at various magnification settings, having a working distance of 10 mm.

Energy dispersive X-ray (EDX) spectroscopy is valuable for quantifying the weights and atomic percentages of constituents present on the external surface of natural fibers. Every element of the fiber has a distinct peak that is utilized to compare the elements. Utilizing an INCA PentaFETx3 model energy dispersive spectroscopy equipment attached to the SEM experimental setup, the element distribution was studied on the *BIF*s surface.

2.4. Chemical analysis

The primary components of plant fibers consist of cellulose, hemicellulose, pectin and lignin, with the proportions of these components varying among different fiber types. In contemporary scientific research, infrared spectroscopy has emerged as one of the most crucial analytical techniques available. One of its paramount advantages is its capability to analyze virtually any sample, regardless of its state. To identify chemical functional groups and evaluate their potential applications, the Attenuated Total Reflectance Fourier Transform Infrared spectroscopy (ATR-FTIR) is the preferred approach among researchers. Experimental tests were conducted using the PerkinElmer RXI FTIR system. ATR-FTIR spectrometer with a 2 cm^{-1} resolution, 32 scans per minute and within the wave number range of 4000-500 $cm^{-1}$was used to identify and categorize the chemical bonds on the *BIF*s. The chemical groups in the *BIF*s grain samples vibrate as they absorb infrared radiation, leaving different frequencies proportional to their strength. Origin software was used to deconstruct the band and make basic modifications to process and study the spectra. Using common test methods, the chemical composition of *BIF*s including cellulose, hemicellulose, lignin, wax, ash, and moisture content was determined. These elements are essential in determining the mechanical characteristics and biodegradability of fiber. The ASTM E1755-01 standard was followed in determining the ash content [38], the Klason lignin method (APPTA P11s-78) was used to determine lignin [39], the Conrad method was used to determine wax [40], the acid treatment followed by an alkali solution (neutral detergent fiber method) to determine hemicellulose [41], and the Kurshner and Hofer method was used to determine cellulose [42].

2.5. Physical analysis

2.5.1. Density measurement

Density measurement is essential for identifying fibers that are natural since it plays a significant role in choosing the right fiber to use for particular structures. The standard procedure for assessing the density of natural fibers involves using a pycnometer setup, following the guidelines of ASTM D 2320-9. To ensure accurate measurements, the required amount of *BIF* was dried at 90 °C for 20 min to remove any moisture content. Short segments of *BIFs* were placed inside a pycnometer (50 ml). Approximately 1 g of it was immersed in ethanol, a liquid with a known density of (0.79 g/cm^3). Measurements were taken in a laboratory environment (27 °C and 50–60 % relative humidity). Density testing was performed using equation (1):

$$\rho_{BIF} = \frac{\Delta m_1}{\Delta m_2 - \Delta m_3} \times \rho_{ethanol} \tag{1}$$

Where Δm_1 refers to the weight difference between the pycnometer without and with *BIF*, Δm_2 denotes the disparity in mass between the pycnometer containing the ethanol solution and the empty pycnometer and Δm_3 represents the *variation* in mass between the pycnometer with the ethanol solution in the presence of *BIF* and without it.

2.5.2. Diameter measurement

Knowing the fiber diameter is crucial as it greatly impacts fiber tensile strength. Measuring fiber diameter is complex due to variations in shape and size among extracted fibers. The profile shapes was identified and the diameter was measured at four random locations on *BI* fiber by using 30 samples. Optical microscopy (MOTIC) has played a vital role in determining the exact values of the diameter, allowing for reliable characterization of fibers. The nominal diameter was calculated as the average diameter value of the *BI* fiber. While this method is somewhat rudimentary, it offers a rapid approximation of fiber diameter. The findings were validated and a computational approach was employed to determine this parameter, assuming a cylindrical shape, through the use of the following formula as per equation (2):

$$D_{BI}(\mu m) = \sqrt{4 * \frac{M}{\pi \rho_{BIF} L}} \tag{2}$$

where L: the length of the fiber (cm), D_{BI} represents the fiber diameter (μm),

M: represents the fiber's mass in grams and ρ_{BIF}: indicates the fiber density (g/cm^3).

2.6. Thermal analysis

2.6.1. Thermal behavior

In order to verify the resistance of natural fibers in composite materials that require high heat resistance, it is necessary to evaluate their thermal stability. Thermal Gravimetric Analysis (TGA) is a valuable method for quantifying a material's major constituents, studying decomposition and evaluating thermal stability. In this study, TGA analysis of *BI* fibers was conducted using an SDT Q600 V20.9 Build device. The fiber bundles were cut into small pieces, dried for 1 h at 70 °C, and then ground into fine powder using a Spex Mixer Mill. An alumina saucepan containing a 36.8 mg dried *BIF* sample was put inside a thermal analyzer. The spectrum was recorded within a temperature range of 26.79 °C–600 °C at a constant heating rate of 10 °C/min. To ensure the preservation of an inert atmosphere within the furnace throughout the experiment, a continuous supply of high-purity N_2 gas was maintained at a rate of 20 ml/min. This test was conducted under controlled atmospheric conditions with a temperature of 30 °C and 65 % relative humidity.

2.6.2. Kinetic activation energy

The activation energy (Ea) represents the minimal energy needed for fiber decomposition and can be mathematically determined by analyzing the slope derived from the curve plot of equation (3). The Borido's equation is used to express the kinetic activation energy (Ea) for untreated *BIFs* as follows:

$$\log\left[\frac{-\log(1-\alpha)}{T^2}\right] = \log\frac{AR}{\beta Ea}\left[1 - \frac{2RT}{Ea}\right] - \frac{Ea}{2.303\,RT} \tag{3}$$

Where α is the sample decomposing at the moment t provided by $\alpha = \frac{W_0 - W_t}{W_0 - W_f}$.

W_0 is the sample's initial weight (before the decomposition reaction begins), W_t is the sample's weight at any given temperature, W_f is the sample's final weight after the reaction is finished, A is the frequency factor, β is the heating rate along a straight line, R is the gas constant and T is the temperature in degrees absolute.

2.7. Crystalline analysis

The importance of using X-ray diffraction lies in determining the crystalline and amorphous nature of materials within natural fibers. XRD technique was used to identify the crystal size (CS) and crystallinity index (CI) of the particular fibers. X'Pert-PRO PANalytical spectrometer with a CuK radiation source operating at 30 mA and a scan speed of 2 min^{-1} was utilized in this

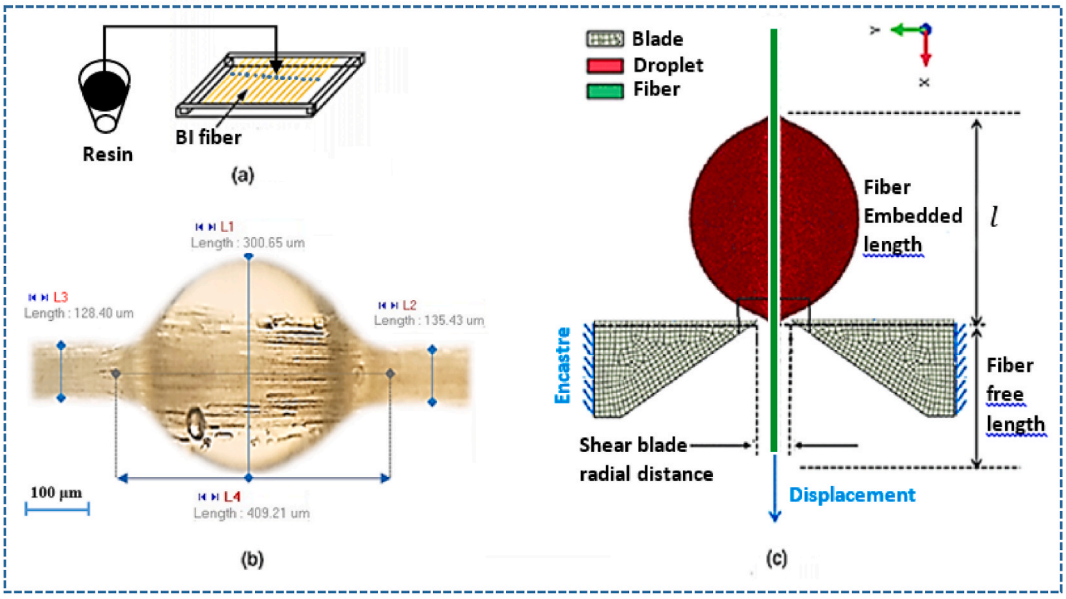

Fig. 3. Droplet test of *BIFs*: (**a**) Fiber impregnation, (**b**) Micrograph specimen and (**c**) Microdroplet test.

investigation. With an applied voltage of 40 kV, using a 0.05° step size and a constant temperature of 25 °C, the range of 2θ is between 10° and 80°. The XRD spectrum scan and data processing of the *BI* fibers were analyzed by identifying individual crystalline and amorphous peaks through a curve fitting process applied to the diffraction intensity profile. The crystallinity index (CI) of *BIF* was determined by applying equation (4) and employing Origin Software (2021) to locate the peak. Assuming a function that is Gaussian for each peaking, with an F-number more than 1000, corresponding to an R_2 greater than 0.9559. These factors are important because they have a large influence on the mechanical properties of fibers.

$$CI = \left\{ 1 - \left(\frac{I_{amorphous}}{I_{crystalline}} \right) \right\} * 100 \tag{4}$$

$I_{crystalline}$ corresponds to the highest intensity observed in the crystalline peak at 2θ angles of 21–22°, while $I_{amorphous}$ indicates the lowest intensity observed in the amorphous peak within the range of 2θ angles from 16 to 17°. By applying Scherrer's formula, which is represented in Equation (5), it was possible to estimate the *BI* fiber's Crystal Size (CS). Scherrer's correction factor (k = 0.94), the incoming X-Ray radiation wavelength (λ = 0.1542 nm), the Bragg angle (θ) were all used in this computation and the peak's full width half maximum (β).

$$CS = \frac{K\lambda}{\beta \cos \theta} \tag{5}$$

2.8. Mechanical property analysis

2.8.1. Mechanical test

The plant fiber cell wall comprises two distinct sections: the primary cell wall, characterized by an irregular network of densely packed cellulose micro-fibrils and the secondary wall, which consists of three layers known as S_1 (outer), S_2 (middle) and S_3 (inner) layers [43]. Tensile test results for plant fibers often exhibit variations due to numerous factors such as fiber extraction method, age of plant, testing conditions, diameter variations and the presence of surface defects. To ensure the reliability and reproducibility of the results, 30 samples of *BIFs* were chosen for tensile property analysis. Tensile testing was conducted following ASTM C1557-14 standard guidelines, utilizing a 40 mm gauge length for single fibers, a crosshead speed of 2.5 mm/min and a 2.5 kN load cell. These tests were carried out under controlled conditions, maintaining a constant temperature of 25 °C and a humidity level of 62 %, ensuring a consistent and accurate experimental setup.

2.8.2. Micro-droplet test

A popular micromechanical technique for evaluating the interfacial characteristics between the resin matrix and single filaments is the microdroplet test [44]. This test involves the formation of an ellipsoidal polymer droplet on the fiber's surface, as illustrated in Fig. 3a. Before testing, the droplet's geometry was examined using an optical microscope (MOTIC), as depicted in Fig. 3b. Microdroplet testing on *BI* fibers was conducted using the Instron ZWICK Z005 universal tensile strength machine. A pair of knives was positioned on either side of the fiber, near the droplet, to restrict its movement. The blades were then pulled at a rate of 0.5 mm/min until the droplet

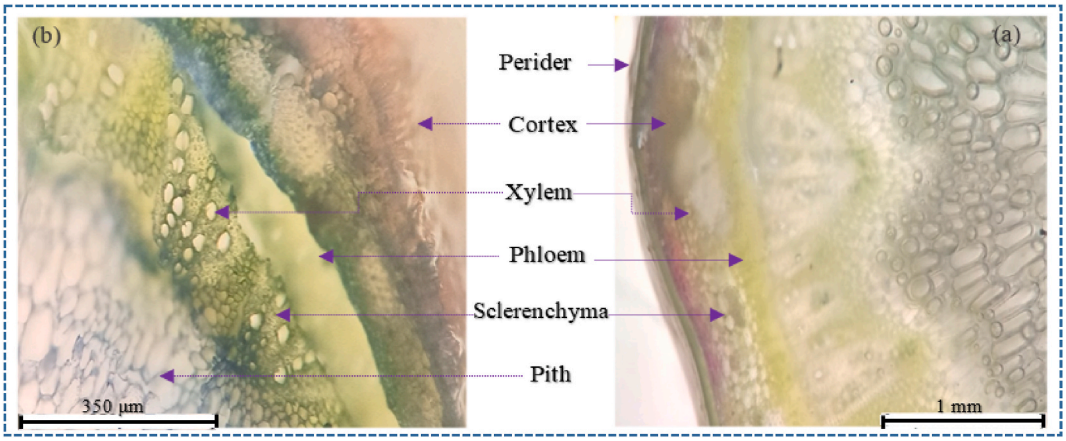

Fig. 4. Transverse optical micrographs of *BI* stem captured at: (**a**) 10 x, and (**b**) 40 x

sheared off. The test setup is shown in Fig. 3c. For IFSS estimation, a minimum of 10 samples were utilized and the average value was subsequently reported. The average IFSS is calculated using the following equation (6) using the peak load and embedded area data:

$$\tau_c = IFSS = \frac{F_{max}}{2\,\pi\, r\, l} \tag{6}$$

Here τ_c: Interfacial shear strength, the strongest pull-out force is referred to as F_{max}, 2r: Fiber diameter and the embedded length is *l*.

2.9. Weibull distribution analysis

The analysis of experimental outcomes obtained from tests conducted on lignocellulosic fibers poses challenges because of the inherent result dispersion characteristic to this fiber type. This variation can be explained to defects within the fiber or on its surface, making it imperative to employ statistical methodologies for assessing its mean mechanical properties. Recently, Weibull analysis has found extensive use in statistically analyzing the mechanical properties of natural fibers. Weibull statistical analysis was performed using both 2 and 3 parameters models to calculate the observed dispersion in the experimental tensile results. The former incorporates parameters for scale and shape, while the latter adds a location parameter, enabling the distribution to shift along the x-axis. Weibull distribution plots were generated and analyzed to represent the average values of mechanical properties and evaluate the variation in fiber strength, strain and Young's modulus. This statistical analysis was conducted using Minitab 19. The three-parameter Weibull cumulative distribution function is as follow equation (7):

$$F(x) = 1 - \mathrm{Exp}\left[-\left(\frac{x - k_0}{k}\right)^n\right] \tag{7}$$

Here, n functions as the Weibull modulus, $k > 0$ relates to the scale parameter and the parameter k_0, which represents the average value of x, should also be acknowledged. Keeping in mind that x, k, k_0 and n are all real numbers greater than zero. To ensure result validity, evaluations of variables were conducted at a 95 % confidence level and developed a two-parameter Weibull model with the assumption that the threshold is zero, which means that k_0 equals zero.

3. Results and discussion

3.1. Anatomical analysis

The stem of a plant is often rich in fiber, commonly referred to as the phloem, where they are present in bundles of elementary fibers encircling the core tissues, known as plant fibers. An in-depth examination of the mature *BI* stem was conducted using an optical microscope, as seen in Fig. 4, to analyze its anatomical structure. The *BI* stem's anatomical arrangement reveals a typical stem structure, characterized by a less distinct peripheral epidermal layer, followed by a cortex housing distinctive phloem and xylem, shown in Fig. 4a. The stem structure has a strongly undulating periderm on the outside, followed by a varying thickness epidermis and cortex. The outermost layer is the epidermis, covered by a thin cuticle. Both the epidermis and the sclerenchyma are observable see Fig. 4a and b, with cellulose fibers bundled together by phloem tubes in the middle and xylem. They manifest as circular cells joined through layers of sclerenchyma, comprising the fundamental components (hemicellulose, pectin and lignin). Whereas the xylem forms an inner conical segment. The phloem component is broad and compact, containing sieve elements and parenchymatous cells (Fig. 4a). This anatomical feature resembles findings from other studies conducted by various researchers on different plant species [25,45].

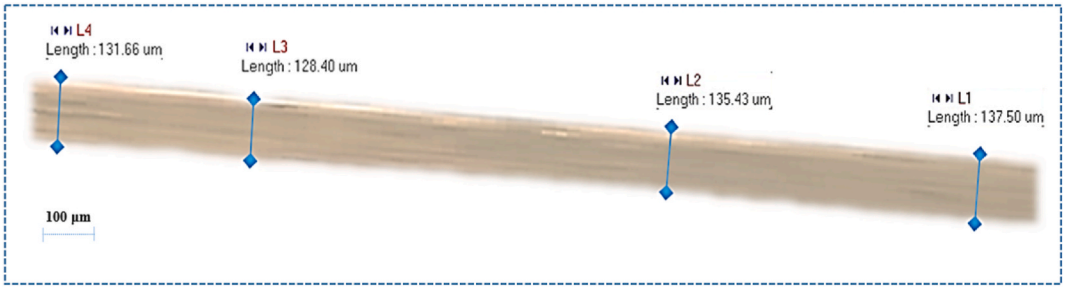

Fig. 5. Ideal microscope image for diameter measurement.

3.2. Diameter and density analysis

Analyzing natural fibers physically involves evaluating both their diameter and density. Measuring the diameter of bio-fibers is a complex task due to the variability in their outer profile. Consequently, taking measurements at four different positions ensures greater accuracy. The diameter of the *BI* Fiber was measured using an optical microscope (Fig. 5), showing that the results obtained are very close to the average calculated diameter of 145.58 ± 7.897 µm. This measurement provides crucial insights into the nature of physical properties, which can significantly influence their mechanical properties. Additionally, it aids in the selection of new natural fibers with lower densities, contributing to lightweight composite materials. The results of our measurements to obtain the density of *BIFs* yielded a value of 1.065 ± 0.025 g/cm^3, which is relatively light compared to various new and traditional natural fiber sources. This density closely resembles that of natural fibers from *Syagrus Romanzoffiana* (1.23 g/ cm^3) [14], and *Centaurea melitensis* (1.26 ± 0.018 g/ cm^3) [25]. Conversely, it is lower than fibers from *Acacia leucophloea* (1.385 g/ cm^3) [23] and *Derris scandens stem* (1.43 ± 0.018 g/ cm^3) [32], as well as *Saharan Aloe vera* (1.325 g/ cm^3) [46]. However, compared to fibers from *Areca catechu* L. (0.75 ± 0.05 g/ cm^3) [47] and *Dracaena reflexa* (0.79 g/ cm^3) [48], *BIFs* exhibit higher density. This density is lower than that of synthetic fibers such as glass and carbon fibers [49]. Table 1 offers a detailed comparison of the physical properties of *BIFs*, including fiber diameter and density, with those of other innovative natural fibers.

3.3. Chemical composition analysis

The thermo-mechanical characteristics of natural fibers are widely acknowledged to be related on their chemical composition [38, 53]. Table 2 lists the chemical makeup of *BIFs* as well as other new fibers for comparison. As indicated, *BIFs* have a higher cellulose concentration than many other natural fibers (67.37 %). A greater cellulose concentration in *BIFs* increases the crystalline character of the fiber, resulting in a more hydrophobic nature [54]. As a result, mechanical performances like tensile strength and Young modulus are maintained. The high amounts of lignin in *BIFs* aid in water retention and provide protection against biological assaults; nevertheless, excessive lignin concentration can cause structural degeneration [55]. *BIFs* contain a modest 10.02 % lignin, Furthermore, it was shown that this novel fiber contains 12.23 % of hemicellulose. Additionally, *As shown in Table 2, the amount of wax was 0.9 %. This ratio may not really affect the quality of fiber/matrix adhesion. Manimaran* et al. [50]. *showed that whenever the quantity of wax is very limited (i.e. 0.18 %), a better bond between these fibers and the polymer matrices can be favored.* The thermally stable nature of *BIFs* is ensured by the ash content of 1.8 % and moisture contents are 7.48 %.

Compared to various research findings, the cellulose content in *BIFs* (67.37 %) is comparable to that of *Perotis indica* fiber (68.4 %) [22] and *Epipremnum aureum stem* fiber (66.34 %) [56], but higher than that of *Ficus Carica* fiber (63.17 %) [26]. In terms of lignin content, *BIFs* (10.02 %) resemble *Sida mysorensis* fiber (9.46 %) [57] but exhibit a lower content than *Dichrostachys Cinerea* fiber (16.89 %) [55]. The presence of higher levels of wax and moisture can impede the bonding between the fiber and matrix in composite material preparation [59]. Therefore, a lower wax content is preferred, and *BIFs* maintain a favorable (0.9 %), contrasting with *Trachelospermum jasminoides* fiber (2.0 %) [29].

3.4. ATR-FTIR spectral analysis

ATR-FTIR spectroscopy was used to characterize the basic components of natural fibers and the functional group of each. Fig. 6 depicts the functional groups of *BIFs* within the spectral range of 4000- 500 cm^{-1}. The spectrum reveals several noteworthy absorption bands within specific wavenumber ranges. Notably, a broad absorption range from 3125 to 3575 cm^{-1} is observed, with a prominent peak at 3329 cm^{-1}, signifying the O–H stretching vibration within the cellulose structure of *BI* [60]. In the range of 2915–2940 cm^{-1}, a peak at 2924 cm^{-1} is attributed to the asymmetric C–H stretching vibration originating from the CH and CH_2 groups, respectively [61]. Around 2100 to 2140 cm^{-1}, another peak emerges at 2100 cm^{-1}, indicating the aromatic plane deformation and the stretching vibration of C=C bonds connected to the lignin components of *BIFs* [62]. At 1730 cm^{-1}, an absorbance band is evident, resulting from the stretching vibration of (C = O) carbonyl groups present in hemicellulose, lignin, and extractives [63]. A peak at 1590 cm^{-1} is associated with the C=C stretching vibration specific to lignin [64]. The absorbance band at 1410 cm^{-1} is linked to the symmetric bending of CH_3 and CH_2 groups found in cellulose [45]. In the range of 1315–1350 cm^{-1}, a peak at 1315 cm^{-1} corresponds to the

Table 1
Properties of *BIF*s compared to those of other natural fibers.

Natural fiber	Physical properties			Thermal properties			References
	Diameter (μm)	Density (g/ cm^3)		Thermal stability (°C)	Maximum degradation temperature (°C)	Activation energy E_a (kJ/mol)	
Bassia indica	145.58 ± 7.89	1.06 ± 0.025		260.24	321.23	93.78	Current study
Syagrus Romanzoffiana	142	1.23		220	352	64.53	[14]
Acacia leucophloea	168.50	1.385		100	387	73.10	[23]
Centaurea melitensis	187.11 ± 60.41	1.26 ± 0.018		210	317.86	–	[25]
Derris scandens stem	158–169	1.43 ± 0.018		230	332	73.2	[32]
Saharan Aloe vera	80.61	1.325		225	350	60.20	[46]
Areca catechu L	395 ± 17	0.75 ± 0.05		240	325.80	64.54	[47]
Dracaena reflexa	176.20	0.790		232.32	348.78	68.78	[48]
Althaea officinalis L.	156–194	1.180		220	344	–	[50]
Typha Augustata	105 ± 10.15	1.015		298.48	450	67.99	[51]
Hierochloe Odarata	136.71 ± 4.34	1.16 ± 0.02		–	352.20	–	[52]
Natural fiber	Crystalline properties			Tensile properties			References
	Peak position (°)	Crystalline index (%)	Crystallite size (nm)	Tensile strength (MPa)	Young's modulus (GPa)	Elongation at break (%)	
Bassia indica	16.15/21.72	40.12	02.23	417.50 ± 7.08	17.46 ± 1.55	1.17 ± 0.02	Current study
Syagrus Romanzoffiana	15.81/21.80	40.81	11.40	671	415	1.84	[14]
Acacia leucophloea	14.80/22.20	51.00	15.00	317–1608	8.41–69.61	1.38–4.24	[23]
Centaurea melitensis	–	47.69	16.92	336.87 ± 59.94	23.87 ± 5.21	1.27 ± 0.36	[25]
Derris scandens stem	15.34/22.82	58.15	11.92	437–785	4.80–22.07	3.34–9.11	[32]
Saharan Aloe vera	17.8/22.59	56.50	05.72	805.50	42.29	2.39	[46]
Areca catechu L	-/20.12	55.50	07.90	322.829 ± 67	3.115 ± 2.31	10.23 ± 2.75	[47]
Dracaena reflexa	15.58/22.31	57.32	19.01	829.60	46.37	2.95	[48]
Althaea officinalis L.	15.70/22.30	68.00	02.40	415.20	65.40	3.90	[50]
Typha Augustata	15.39/23.19	65.16	06.40	665 ± 7	27.45 ± 3	3.12 ± 0.5	[51]
Hierochloe Odarata	16.12/22.12	63.80	–	105.70	2.56	2.40	[52]

Table 2
Chemical composition of *BIF*s compared to those of other natural fibers.

Natural fibers	Cellulose (wt %)	Hemi-cellulose (wt %)	Lignin (wt %)	Wax (wt %)	Moisture content (wt %)	Ash (wt %)	References
Bassia indica	67.37	12.23	10.02	0.9	7.48	1.8	Current study
Perotis indica	68.4	15.7	8.35	0.32	9.54	4.32	[22]
Ficus Carica	63.17	12.08	13.7	0.42	9.07	1.05	[26]
Trachelospermum jasminoides	62.7	14.5	4.1	2.0	7.8	1.5	[29]
Dichrostachys Cinerea	72.4	13.08	16.89	0.57	9.82	3.97	[55]
Epipremnum aureum stem	66.34	13.42	14.01	0.37	7.41	4.61	[56]
Sida mysorensis	53.36	15.23	9.46	0.86	10.48	3.33	[57]
Pergularia Tomentosa L.	43.8	16	8.6	1.88	8.5	2.74	[58]

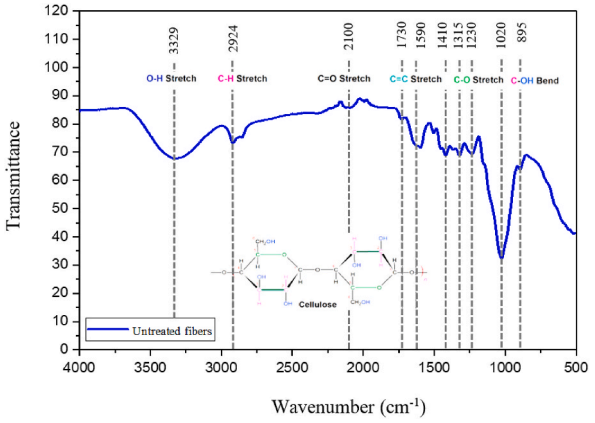

Fig. 6. ATR-FTIR spectra for *BIF*s in its raw state.

Table 3
ATR-FTIR vibrational spectra for *BIF*s.

Infrared limits	Bands position in this work cm^{-1}	Vibrations mode(s)	Source(s)	Ref
3125–3575	3329	Hydrogen bonded O–H stretching.	Cellulose, Hemicelluloses	[60]
2915–2940	2924	C–H stretching vibration-asym.	Cellulose, Hemicelluloses	[61]
2100–2140	2100	C–H stretching vibration.	Hemicellulose	[62]
1600–1740	1730	C=O stretching & bending.	Hemicellulose, lignin and extractives	[63]
1580–1600	1590	C=C stretching vibration.	lignin	[64]
1400–1420	1410	C–H in-plane deformation vibration (CH_2 and CH_3).	Cellulose	[45]
1315–1350	1315	C–O groups of the aromatic ring in polysaccharides	lignin compounds, Cellulose, Hemicelluloses	[65]
1225–1265	1230	= C–O and C–O–C stretching vibration.	Cellulose, Hemicelluloses	[66]
1000–1040	1020	C–O–C bridge stretching.	Cellulose, Hemicelluloses	[67]
880–900	895	**β**-glycosidic linkages between the monosaccharides	Cellulose, Hemicelluloses	[13]

bending vibration of C–H and C–O bonds in the aromatic ring groups of the polysaccharides [65]. At 1230 cm^{-1}, within the range of 1225–1265 cm^{-1}, a peak signifies the stretching vibration indicative of = C–O bonds in the acetyl group of hemicellulose [66]. An intense peak at approximately 1020 cm^{-1} is observed between 1000 and 1040 cm^{-1}, which relate to stretching vibrations of generated by the C–O and O–H in the lignin contained in the fiber [67]. Last but not least, that band at 895 cm^{-1} is connected to the cellulose and hemicellulose β-glycosidic contribution [13]. This analysis of the results shows that the IR bands display absorption patterns akin to those observed in most of the analyzed natural fibers. This study involved an examination of *BIF*s and the presence of significant components was verified using infrared spectroscopy. Table 3 provides an overview of the primary spectral bands and their associated functional groups as determined through ATR-FTIR spectrum analysis of *BIF*s.

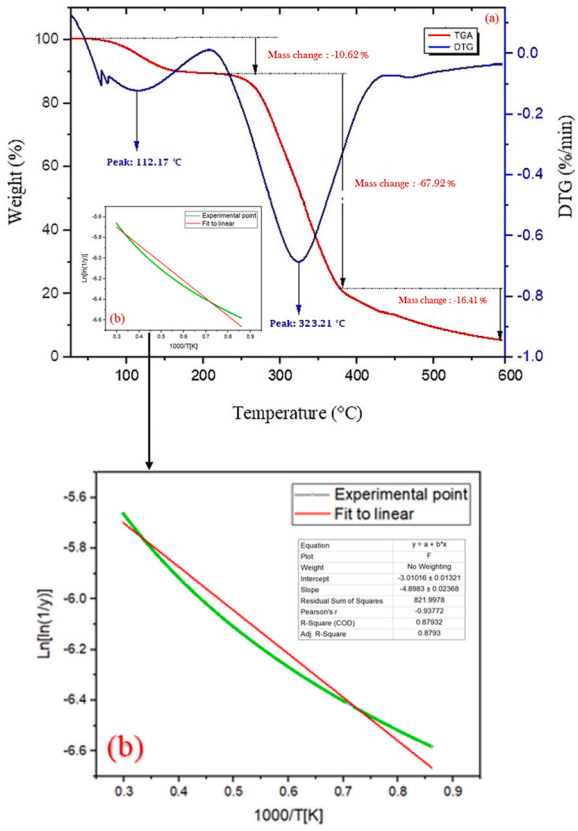

Fig. 7. (**a**) TGA and DTG thermograms of *BIFs* and (**b**) Broido's Plot of *BIFs*.

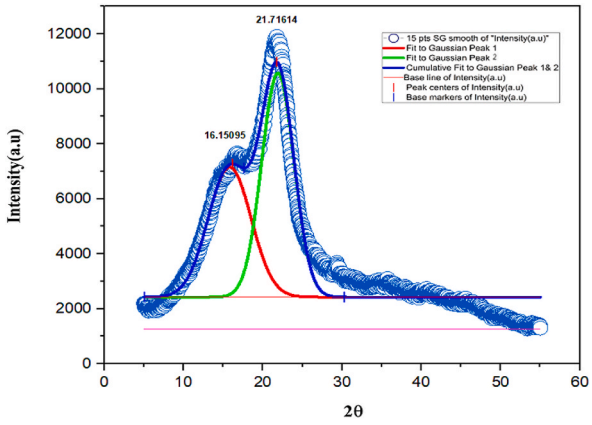

Fig. 8. X-ray diffraction of *BIFs*.

3.5. *Thermogravimetric analysis (TGA)*

Typically, bio-fiber-reinforced thermoplastic composites are produced at elevated temperatures. Consequently, it is crucial to assess the thermal stability of bio-fiber across different temperature settings to: (I) determine the precise temperature range suitable for composite manufacturing and (II) prevent any degradation of fiber properties. The curves for *BIF's* thermogravimetric (TGA) and first derivative (DTG) measurements are shown in Fig. 7a. At 112.17 °C, the fiber begins to decompose somewhat, resulting in a weight reduction of 10.62 % caused by the elimination of moisture in the fiber, confirming its hydrophilic nature. Remarkably, no weight loss is evident until the temperature reaches 210 °C, indicating the high level of heat stability achieved by the fibers up to that point. Subsequently, between 210 °C and 400 °C, there is a substantial combined degradation involving cellulose, hemicellulose, and a significant quantity of unstable materials, with a peak degradation temperature at 323.21 °C and a weight loss of 67.92 %. The ultimate

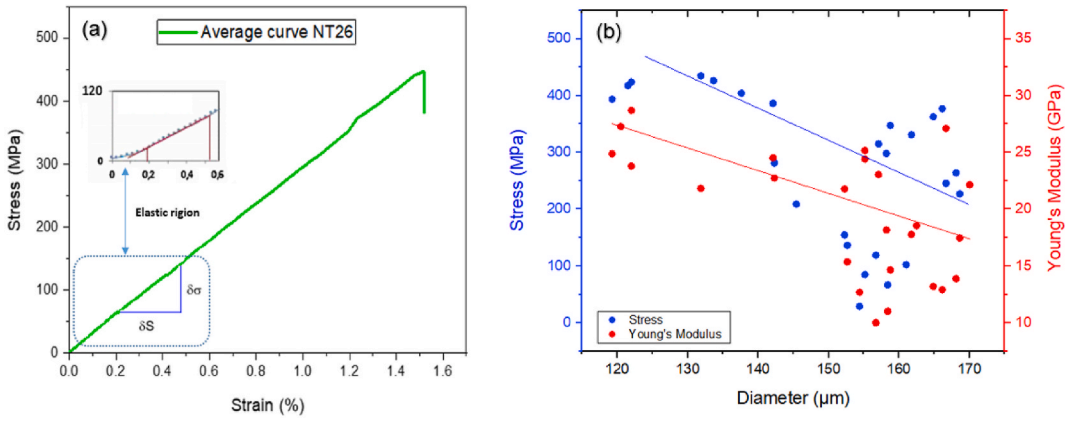

Fig. 9. (**a**) Standard stress-strain curve of *BIF*s with a zoomed-in view of the elastic region and (**b**) Stress at break and young's as a function of fiber diameter.

weight loss of 16.41 % indicates the decomposition of additional substances in the *BIF*s, such as wax, lignin and the oxidative degradation of charred residue. Lignin, a highly complex and undesirable polymer, necessitates more time and higher temperatures for degradation due to its intricate nature. The lignin breakdown process begins at temperatures over 200 °C, while it mostly takes place between 225 °C and 600 °C. Ultimately, a residual weight of 5.05 % remains at 600 °C. TGA data can be analyzed using various methods to determine kinetic parameters. In Fig. 7b, the activation energy was determined from the slope a value resulting in an activation energy of 93.78 kJ/mol. Moreover, the obtained value of activation energy (Ea) of *BI* fiber was in the range of 60–170 kJ/mol [64]. This analysis of *BIF*s thermal decomposition suggests that it is suitable as a reinforcement material for composites at working temperatures not exceeding 210 °C. Table 1 provides a summary and comparison of the properties of the natural fibers examined by the researchers with the thermal properties of *BIF*s.

3.6. X-ray diffraction analysis (XRD)

The XRD spectrum of *BIF's* sample, as depicted in Fig. 8, displays two distinct peaks. The amorphous percentage of hemicellulose and lignin is represented by the first peak, which appears at $2\theta = 16.15°$ (related to crystallographic plane 100) and by the second peak, which is represented by cellulose and is located at $2\theta = 21.71°$ (related to crystallographic plane 002) [68]. These results demonstrate that the *BI* fiber bundle is semi-crystalline and these peaks may also sometimes related to the crystallographic planes (200) and ($1\ \bar{1}\ 0$), respectively. The increase in the index values a result of enhancements in cellulose chain packing, elimination of non-cellulosic materials and the extraction of water through the disruption of hydrogen bonds, leading to the reshaping of crystalline regions. The cellulose fibers' crystallinity index is a crucial parameter due to its substantial influence on mechanical properties. It is calculated by dividing the total area by the area of all crystalline peaks. Additionally, Scherrer's equation is used to calculate the Crystallite Size, which indicates the typical size of a single crystal.

The crystallinity index of *BIF* was determined to be 40.12 %, which is higher than that of several other bio-fibers, *Cissus vitiginea* stem (30.5 %) [31], *Cyperus compactus* (37.08 %) [24], but lower than that of *Acacia leucophloea* (51.00 %) [38], *Derris scandens* stem (58.15 %) [32] and *Typha Augustata* (65.16 %) [51]. Furthermore, the crystallite size (CS) of *BIF* was calculated as 2.23 nm. The crystallite size value of *BI* Fiber is comparable to that of *Althaea officinalis* L. fiber (2.40 nm) [50], *Saharan aloe vera* fiber (5.72 nm) [46], *Syagrus Romanzoffiana* fiber (11.40 nm) [14], and *Centaurea melitensis* fiber (16.92 nm) [25]. These identified crystalline properties of *BIF*s are reliable enough to make the fiber an excellent candidate for usage as reinforcing in materials made from composites. Table 1 represents a comparison of the crystal properties with several natural fibers.

3.7. Tensile analysis

In this investigation, and in order to obtain precise assessments of mechanical properties, a total of thirty fibers were randomly selected and subjected to static tensile testing with a gauge length of 40 mm. Fig. 9a displays a typical stress-strain curve. This curve illustrates a linear correlation when *BIF*s undergo tensile loading, where the stress increases proportionally to the strain, reaching a maximum value of 1.57 %. Upon reaching failure, all examined fibers exhibit a brittle behavior, resulting in a rapid decline in stress. The tensile strength of *BI* Fiber was determined to be 417.50 ± 7.08 MPa, which is lower than that of *Dracaena reflexa* fiber (829.60 MPa) [48] but higher than *Areca Catechu* L. (322.829 ± 67 MPa) [47], *Hierochloe Odarata* fibers (105.70 MPa) [52], and roughly similar to *Althaea officinalis* L fibers (415.20 MPa) [50]. Nevertheless, *BI* fiber exhibits reasonable properties suitable for low-cost applications. The findings showed that the Young's modulus was 17.46 ± 1.55 GPa and the strain at failure was 1.17 ± 0.02 %, the mechanical properties of *BIF*s are compared to other natural fibers (Table 1). The relationship between tensile strength and Young's modulus and the diameter of the fibers employed in the tests is shown in Fig. 9b. This comparison allows for the evaluation of *BIF*s' mechanical properties. It is noticeable that as the fiber diameter increases, both tensile strength and Young's modulus decrease.

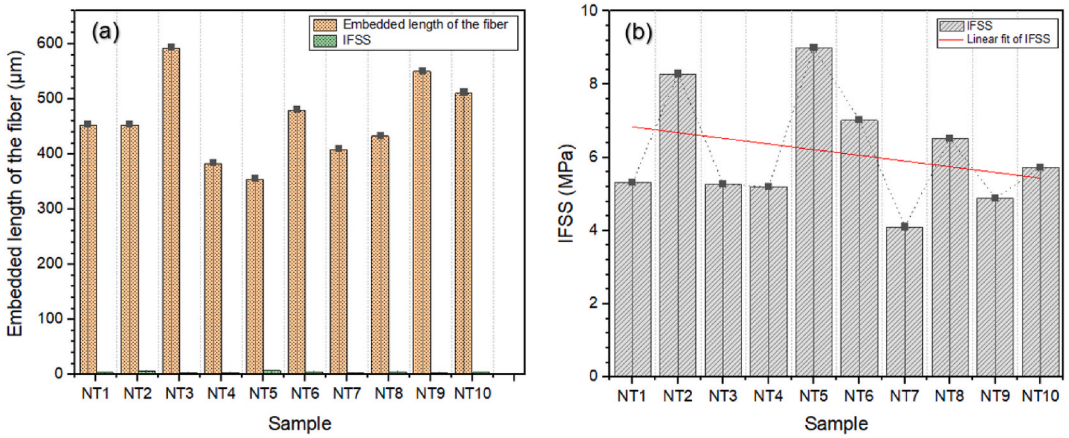

Fig. 10. (**a**) Each sample's apparent IFSS and embedded fiber length, and (**b**) calculated IFSS.

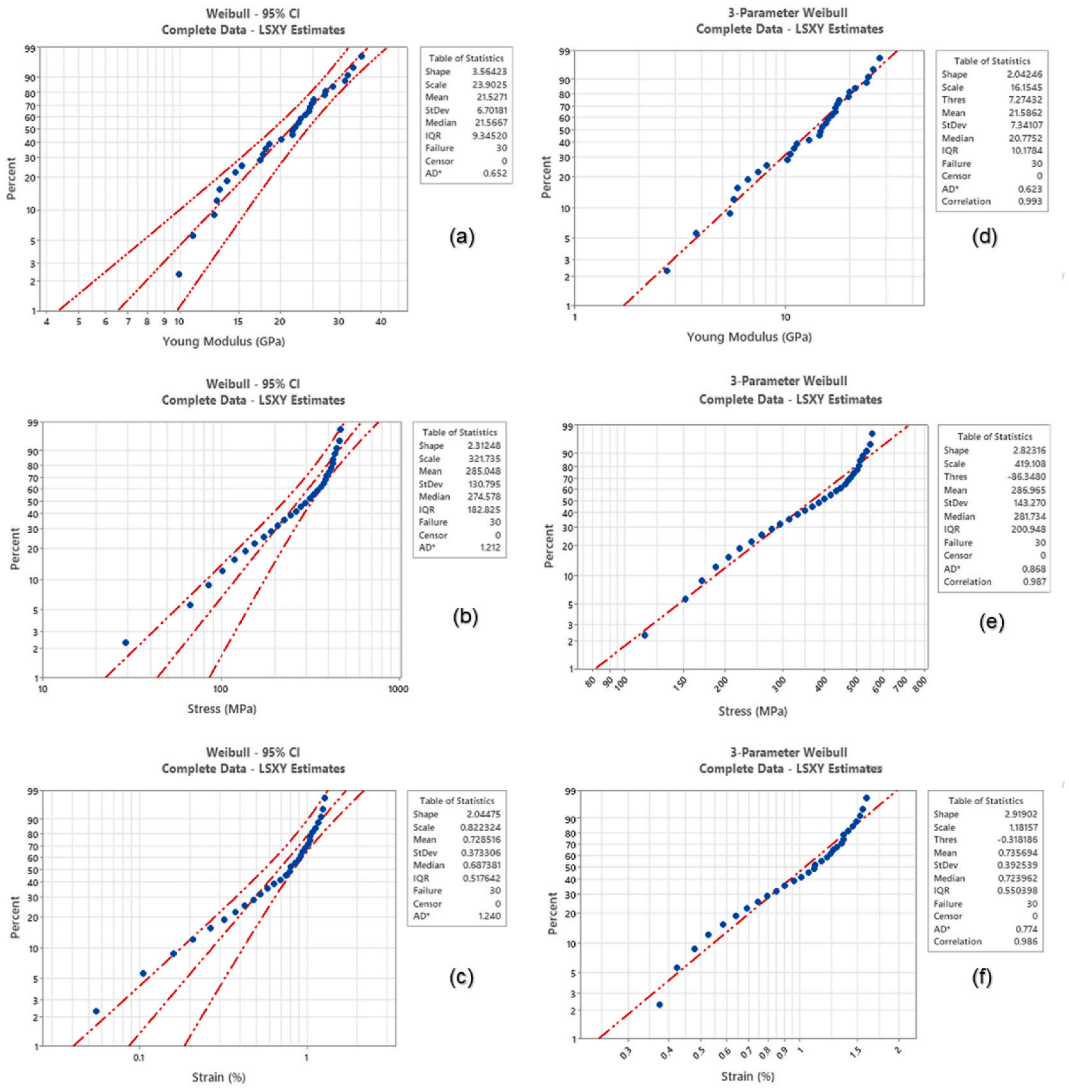

Fig. 11. Weibull distribution with both two parameters and three parameters for the tensile strength, Young's modulus and strain at break.

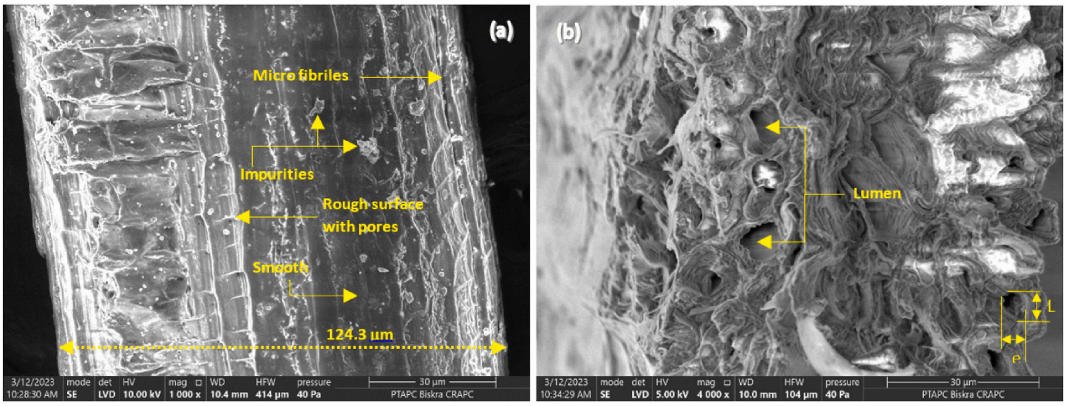

Fig. 12. SEM micrographs of *BIFs*: (**a**) longitudinal view (1000x) and (**b**) cross-sectional view (4000x).

Additionally, Young's modulus and tensile strength values exhibit variability due to various random variables, including test conditions, fiber age, region and extraction method. Consequently, the utilization of statistical approaches is essential to assess the average tensile properties effectively.

Microdroplet testing technique was employed to measure shear strength and calculate the interfacial force between epoxy/*BI* fibers, as illustrated in Fig. 3b. The outcomes were plotted on a bar graph in Fig. 10a, depicting the interfacial shear strength (IFSS), against the length of the fibers embedded in each sample. Notably, observed a significant variation in IFSS values based on the length of the droplet immersed on the surface of the *BIFs*. This variation is also evident in the IFSS graph derived from the test results. The average IFSS value was determined to be 6.99 ± 1.10 MPa (seen in Fig. 10b). Our results highlight that differences in interfacial shear strength are influenced not only by the adhesive area between resin and fiber, but also by various factors including natural fiber type, surface roughness and diameter variations of ligno-cellulosic fiber. These combined factors contribute to alterations in the mechanical behavior of the fibers. Based on the results obtained, it is reasonable to assert that *BIFs* are suitable for reinforcing polymer composites.

3.8. Statistical analysis

Due to the substantial number of experiments (twenty sample); variations in the mechanical properties were observed, necessitating a statistical analysis. This methodology has been employed by several authors in previous studies [25,45,48,69]. The analysis of mechanical properties was conducted using the commercial software Minitab 19, employing the Weibull distribution with both two parameters and three parameters to identify the most appropriate distribution. Fig. 11 shows the *BIFs*' stress, Young's modulus and strain at break distributions using Weibull statistics. Specifically, Fig. 11a, b and 11c, as well as Fig. 11d, e and 11f, compare the types of probability distributions. We utilized two-parameter and three-parameter Weibull LSXY (least squares) statistical distribution curves to analyze the obtained mechanical properties at a 95 % confidence level. It is significant to note that the two-parameter Weibull distribution's Young's modulus and strain were determined to be 23.9 GPa and 0.82 %, respectively. While in the three-parameter Weibull distribution, they were measured as 16.15 GPa and 1.18 %, respectively. The tensile test results were derived from our experiments (30 sample) closely align with the Weibull distribution, having a correlation value of around $R_2 = 0.98$, showing high agreement. Clearly, the three-parameter Weibull distribution yields mechanical properties that closely match the experimentally obtained average values, making it the most suitable for estimating the stress in *BIFs*. For instance, the predicted tensile properties closely align with the experimental results, with a value of approximately 419.10 MPa compared to the experimentally obtained value of 417.50 MPa. This agreement between predicted and experimental data demonstrates the Weibull function's utility in statistically characterizing the mechanical failure of ligno-cellulosic fibers.

3.9. Scanning electron microscope analysis (SEM)

Surface morphology analysis is critical since it yields valuable insights into the potential utilization of fibers as reinforcement in diverse composite materials. SEM images offer precise details regarding the surface topography of *BIFs*. For longitudinal views, SEM micrographs were captured at 1000x magnification, while for cross-sectional views, they were taken at 4000x magnification. Fig. 12a displays SEM images that depict the morphology of the extracted *BIFs*, offering a glimpse into their physical structure. Importantly, these images highlight a distinct feature known as 'wavy patterns,' which arise from variations in the diameters of individual fibers. These patterns facilitated the measurement of the *BIF* bundle's diameter, determined to be 124.6 µm. Moreover, the presence of voids and cavities explains the rough surface characteristics of *BIF*. These fibers include bumps and inclusions on their surfaces, which enhances their adherence to the polymer matrix. In Fig. 12b, the cross-section of the fiber appears uniform with minimal variation. Within each elementary fiber, there exists a central hollow space referred to as the lumen, which possesses a slightly oval shape (with dimensions L = 6 µm and e = 4 µm) and serves a vital function in facilitating the movement of water and nutrients along the fiber [70]. Fig. 12b also display a multicellular surface structure distinguished by constituents such as cellulose. Furthermore, it is coated with

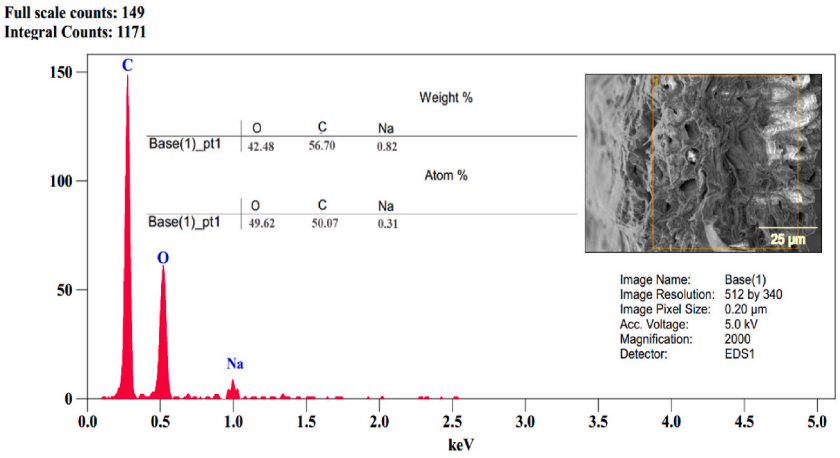

Fig. 13. EDX analysis of the *BIF*s.

various compounds, including hemicellulose, starch grains, lignin, wax and pectin, which are common characteristics of *BIF*s. This composition influences the mechanical properties and interfacial bonding in bio-composites.

3.10. Energy dispersive X-ray analysis (EDX)

The elemental quantitative examination of *BIF*s is depicted in Fig. 13 in terms of atomic and mass percentages, aided by an energy dispersive spectroscope. Significant peaks in the EDX plot revealed the presence of important elements on the surface of *BIF*s, especially carbon, oxygen, and sodium. aligning with the typical composition of cellulosic materials [31]. Among the detected peaks, carbon and oxygen were the most dominating components. *BIF*s have a surface composition of 56.70 wt% carbon (50.07 at.%) and 42.48 wt% oxygen (49.62 at.%). The higher concentration of carbon and oxygen atoms guarantees that the surface of the *BIF*s includes less lignin [71]. *BIF*s, in addition to C and O elements, include 0.82 wt% Sodium (0.31 at.%) on their surface.

4. Conclusion

In this research, we conducted comprehensive characterizations of a novel lignocellulosic natural fiber derived from the *Bassia Indica* plant. The evaluation includes analyzing the fibers' anatomical structure, chemical composition through ATR-FTIR, crystalline properties via XRD, thermal behavior using TGA, mechanical properties through tensile testing and examining their surface morphology. This comprehensive analysis aims to provide insights into the fibers' thermal, physical and mechanical characteristics, helping researchers make informed decisions regarding their potential application in polymer composites.

The *BIF*s fiber exhibited an average density of 1.065 ± 0.025 (g/cm^3) and a diameter of 145.58 ± 7.89 µm. The crystallite size of *BI* Fiber was determined to be 2.23 nm. Furthermore, analysis shows that *BIF*s are rich in cellulose content (67.37 %). TGA analysis indicated that *BIF*s remain thermally stable up to 260.24 °C. The tensile strength, Young's modulus and elongation at break for *BIF*s were measured at 417.50 ± 7.08 MPa, 17.46 ± 1.55 GPa, and 1.175 ± 0.029 %, respectively. We have established that *BIF*s represent a practical and environmentally sustainable choice across diverse industries, encompassing the fields of composite materials.

CRediT authorship contribution statement

Djamila Kouidri: Writing – original draft, Software, Resources, Methodology, Investigation, Funding acquisition, Formal analysis, Data curation, Conceptualization. **Mansour Rokbi:** Writing – original draft, Visualization, Validation, Supervision, Project administration, Methodology, Investigation, Funding acquisition, Formal analysis, Data curation, Conceptualization. **Zine Elabidine Rahmouni:** Writing – original draft, Visualization, Validation, Methodology, Investigation, Funding acquisition, Formal analysis, Data curation, Conceptualization. **Younes Kherbiche:** Writing – review & editing, Visualization, Validation, Software, Funding acquisition, Formal analysis, Data curation, Conceptualization. **Samira Bouchareb:** Writing – review & editing, Visualization, Validation, Methodology, Conceptualization. **Sanjay Mavinkere Rangappa:** Writing – review & editing, Validation, Methodology, Investigation, Formal analysis, Conceptualization. **Suchart Siengchin:** Writing – review & editing, Validation, Methodology, Formal analysis, Conceptualization.

Declaration of competing interest

The authors declare the following financial interests/personal relationships which may be considered as potential competing interests

Acknowledgements

The authors would like to thank the engineers of Center for Scientific and Technical Research and Physical and Chemical Analysis of the Biskra- Algeria. The authors would like to thank the National Science, Research and Innovation Fund (NSRF) (Fundamental Fund 2024), and King Mongkut's University of Technology North Bangkok (Project no. KMUTNB–FF–67-A-03).

References

[1] A. Vinod, M. Sanjay, S. Suchart, P. Jyotishkumar, Renewable and sustainable biobased materials: an assessment on biofibers, biofilms, biopolymers and biocomposites, J. Clean. Prod. 258 (2020) 120978, https://doi.org/10.1016/j.jclepro.2020.120978.
[2] G. Gedik, O. Avinc, Hemp fiber as a sustainable raw material source for textile industry: can we use its potential for more eco-friendly production? Sustainability in the Textile and Apparel Industries, Sourcing Natural Raw Materials (2020) 87–109, https://doi.org/10.1007/978-3-030-38541-5_4.
[3] A. Moshi, S. Madasamy, S. Bharathi, P. Periyanayaganathan, A. Prabaharan, Investigation on the mechanical properties of sisal–banana hybridized natural fiber composites with distinct weight fractions, International Conference On Materials (2019), https://doi.org/10.1063/1.5117941. Manufacturing And Machining 2019 2128.
[4] R. Gopinath, P. Billigraham, T. Sathishkumar, Investigation of physico-chemical, mechanical, and thermal properties of new cellulosic bast fiber extracted from the bark of bauhinia purpurea, J. Nat. Fibers 19 (2022) 9624–9641, https://doi.org/10.1080/15440478.2021.1990180.
[5] C.B. Ayyanar, K. Marimuthu, B. Gayathri, C. Bharathiraj, S.P. Mohan, S. Mr, A. Khan, S. Siengchin, Development and characterization of Hevea brasiliensis particulates filled polyethylene composites, Polym. Compos. 43 (2022) 2047–2054, https://doi.org/10.1002/pc.26519.
[6] A. Vinod, R. Vijay, D.L. Singaravelu, M. Sanjay, S. Siengchin, M. Moure, Characterization of untreated and alkali treated natural fibers extracted from the stem of Catharanthus roseus, Mater. Res. Express 6 (2019) 085406, https://doi.org/10.1088/2053-1591/ab22d9.
[7] M. Sanjay, B. Yogesha, Studies on hybridization effect of jute/kenaf/E-glass woven fabric epoxy composites for potential applications: effect of laminate stacking sequences, J. Ind. Textil. 47 (2018) 1830–1848, https://doi.org/10.1177/1528083717710713.
[8] R. Phiri, S.M. Rangappa, S. Siengchin, D. Marinkovic, Agro-waste natural fiber sample preparation techniques for bio-composites development: methodological insights. Facta Universitatis, Series: Mechanical Engineering 21 (4) (2023 Dec 16) 631–656, https://doi.org/10.22190/FUME230905046P.
[9] S.M. Rangappa, S. Siengchin, J. Parameswaranpillai, M. Jawaid, T. Ozbakkaloglu, Lignocellulosic fiber reinforced composites: progress, performance, properties, applications, and future perspectives, Polym. Compos. 43 (2022) 645–691, https://doi.org/10.1002/pc.26413.
[10] T. Singh, B. Gangil, A. Patnaik, D. Biswas, G. Fekete, Agriculture waste reinforced corn starch-based biocomposites: effect of rice husk/walnut shell on physicomechanical, biodegradable and thermal properties, Mater. Res. Express 6 (2019) 045702, https://doi.org/10.1088/2053-1591/aafe45.
[11] R. Vijay, D.L. Singaravelu, A. Vinod, M. Sanjay, S. Siengchin, M. Jawaid, A. Khan, J. Parameswaranpillai, Characterization of raw and alkali treated new natural cellulosic fibers from Tridax procumbens, Int. J. Biol. Macromol. 125 (2019) 99–108, https://doi.org/10.1016/j.ijbiomac.2018.12.056.
[12] C.E. Okafor, L.C. Kebodi, C.C. Ihueze, S.M. Rangappa, S. Siengchin, U.C. Okonkwo, Development of Dioscorea alata stem fibers as eco-friendly reinforcement for composite materials, Journal of King Saud University-Engineering Sciences (2022), https://doi.org/10.1016/j.jksues.2022.02.003.
[13] N. Lemita, S. Deghboudj, M. Rokbi, F.M.L. Rekbi, R. Halimi, Characterization and analysis of novel natural cellulosic fiber extracted from Strelitzia reginae plant, J. Compos. Mater. 56 (2022) 99–114, https://doi.org/10.1177/00219983211049285.
[14] O. Ferfari, A. Belaadi, A. Bedjaoui, H. Alshahrani, M.K. Khan, Characterization of a new cellulose fiber extracted from Syagrus Romanzoffiana rachis as a potential reinforcement in biocomposites materials, Mater. Today Commun. (2023) 106576, https://doi.org/10.1016/j.mtcomm.2023.106576.
[15] M. Ilangovan, V. Guna, B. Prajwal, Q. Jiang, N. Reddy, Extraction and characterisation of natural cellulose fibers from Kigelia africana, Carbohydrate polymers 236 (2020) 115996, https://doi.org/10.1016/j.carbpol.2020.115996.
[16] R. Muthalagu, V. Srinivasan, S. Sathees Kumar, V.M. Krishna, Extraction and effects of mechanical characterization and thermal attributes of jute, prosopis juliflora bark and kenaf fibers reinforced bio composites used for engineering applications, Fibers Polym. 22 (2021) 2018–2026, https://doi.org/10.1007/s12221-021-1092-9.
[17] M. Kathirselvam, A. Kumaravel, V. Arthanarieswaran, S. Saravanakumar, Characterization of cellulose fibers in Thespesia populnea barks: influence of alkali treatment, Carbohydrate polymers 217 (2019) 178–189, https://doi.org/10.1016/j.carbpol.2019.04.063.
[18] M. Sanjay, S. Siengchin, Exploring the applicability of natural fibers for the development of biocomposites, Express Polym. Lett. 15 (2021) 193, https://doi.org/10.3144/expresspolymlett.2021.17.
[19] P. Madhu, M. Sanjay, P. Senthamaraikannan, S. Pradeep, S. Saravanakumar, B. Yogesha, A review on synthesis and characterization of commercially available natural fibers: Part-I, J. Nat. Fibers (2018), https://doi.org/10.1080/15440478.2018.1453433.
[20] B. Gurukarthik Babu, D. Prince Winston, P. SenthamaraiKannan, S. Saravanakumar, M. Sanjay, Study on characterization and physicochemical properties of new natural fiber from Phaseolus vulgaris, J. Nat. Fibers 16 (2019) 1035–1042, https://doi.org/10.1080/15440478.2018.1448318.
[21] A. Arul Marcel Moshi, D. Ravindran, S. Sundara Bharathi, V. Suganthan, G. Kennady Shaju Singh, Characterization of new natural cellulosic fibers–a comprehensive review, IOP Conf. Ser. Mater. Sci. Eng. 574 (2019) 012013, https://doi.org/10.1088/1757-899X/574/1/012013.
[22] M. Prithiviraj, R. Muralikannan, P. Senthamaraikannan, S. Saravanakumar, Characterization of new natural cellulosic fiber from the Perotis indica plant, Int. J. Polym. Anal. Char. 21 (2016) 669–674, https://doi.org/10.1080/1023666X.2016.1202466.
[23] V. Arthanarieswaran, A. Kumaravel, S. Saravanakumar, Characterization of new natural cellulosic fiber from Acacia leucophloea bark, Int. J. Polym. Anal. Char. 20 (2015) 367–376, https://doi.org/10.1080/1023666X.2015.1018737.
[24] A.K. Bhunia, D. Mondal, K.R. Sahu, A.K. Mondal, Characterization of new natural cellulosic fibers from Cyperus compactus Retz.(Cyperaceae) Plant, Carbohydrate Polymer Technologies and Applications 5 (2023) 100286, https://doi.org/10.1016/j.carpta.2023.100286.
[25] A. Kaldoune, M. Rokbi, Extraction and characterization of novel natural fiber from Centaurea melitensis plant, J. Compos. Mater. 57 (2023) 913–928, https://doi.org/10.1177/00219983221147381.
[26] M. Selvaraj, P. N, R. Pt, B. Mylsamy, Extraction and characterization of a new natural cellulosic fiber from bark of Ficus Carica plant as potential reinforcement for polymer composites, J. Nat. Fibers 20 (2023) 2194699, https://doi.org/10.1080/15440478.2023.2194699.
[27] A.K. Bhunia, D. Mondal, S.M. Parui, A.K. Mondal, Characterization of a new natural novel lignocellulose fiber resource from the stem of Cyperus platystylis R, Br. Scientific Reports 13 (2023) 1–13, https://doi.org/10.1038/s41598-023-35888-w.
[28] A. Belaadi, S. Amroune, Y. Seki, O.Y. Keskin, S. Köktaş, M. Bourchak, A. Dufresne, H. Fouad, M. Jawaid, Extraction and characterization of a new lignocellulosic fiber from Yucca treculeana L. leaf as potential reinforcement for industrial biocomposites, J. Nat. Fibers 19 (2022) 12235–12250, https://doi.org/10.1080/15440478.2022.2054895.
[29] G. Gedik, Extraction of new natural cellulosic fiber from Trachelospermum jasminoides (star jasmine) and its characterization for textile and composite uses, Cellulose 28 (2021) 6899–6915, https://doi.org/10.1007/s10570-021-03952-1.
[30] G. Rajeshkumar, G. Devnani, J.P. Maran, M. Sanjay, S. Siengchin, N.A. Al-Dhabi, K. Ponmurugan, Characterization of novel natural cellulosic fibers from purple bauhinia for potential reinforcement in polymer composites, Cellulose 28 (2021) 5373–5385, https://doi.org/10.1007/s10570-021-03919-2.
[31] S. Chakravarthy, S. Madhu, J.S.N. Raju, J.S. Md, Characterization of novel natural cellulosic fiber extracted from the stem of Cissus vitiginea plant, Int. J. Biol. Macromol. 161 (2020) 1358–1370, https://doi.org/10.1016/j.ijbiomac.2020.07.230.
[32] R. Sarala, Characterization of a new natural cellulosic fiber extracted from Derris scandens stem, Int. J. Biol. Macromol. 165 (2020) 2303–2313, https://doi.org/10.1016/j.ijbiomac.2020.10.086.
[33] A. Othman, Y. Amen, K. Shimizu, A novel acylated flavonol tetraglycoside and rare oleanane saponins with a unique acetal-linked dicarboxylic acid substituent from the xero-halophyte Bassia indica, Fitoterapia 152 (2021) 104907, https://doi.org/10.1016/j.fitote.2021.104907.

[34] S. Qari, E. Tawfik, I. Hammad, Morphological, cytological, physiological and genetic studies of Bassia indica (Amaranthaceae), Gene Conserve 18 (2019), https://doi.org/10.4238/gmr18417.

[35] K. Mayandi, N. Rajini, P. Pitchipoo, J.W. Jappes, A.V. Rajulu, Extraction and characterization of new natural lignocellulosic fiber Cyperus pangorei, Int. J. Polym. Anal. Char. 21 (2016) 175–183, https://doi.org/10.1080/1023666X.2016.1132064.

[36] L.Y. Mwaikambo, M.P. Ansell, Mechanical properties of alkali treated plant fibres and their potential as reinforcement materials. I. hemp fibres, J. Mater. Sci. 41 (2006) 2483–2496, https://doi.org/10.1007/s10853-006-5098-x.

[37] J. Zhang, H. Henriksson, I.J. Szabo, G. Henriksson, G. Johansson, The active component in the flax-retting system of the zygomycete Rhizopus oryzae sb is a family 28 polygalacturonase, J. Ind. Microbiol. Biotechnol. 32 (2005) 431, https://doi.org/10.1007/s10295-005-0014-y.

[38] A.A.M. Moshi, D. Ravindran, S.S. Bharathi, S. Indran, S. Saravanakumar, Y. Liu, Characterization of a new cellulosic natural fiber extracted from the root of Ficus religiosa tree, Int. J. Biol. Macromol. 142 (2020) 212–221, https://doi.org/10.1016/j.ijbiomac.2019.09.094.

[39] Gowda T. Yashas, A. Vinod, P. Madhu, M. Sanjay, S. Siengchin, M. Jawaid, Areca/Synthetic fibers reinforced based epoxy hybrid composites for semi-structural applications, Polym. Compos. 43 (2022) 5222–5234, https://doi.org/10.1002/pc.26814.

[40] Y. Ran, M. Elsayed, M. Eraky, W. Dianlong, P. Ai, Sequential production of biomethane and bioethanol through the whole biorefining of rice straw: analysis of structural properties and mass balance, Biomass Conversion and Biorefinery (2022) 1–13, https://doi.org/10.1007/s13399-022-02548-4.

[41] G.A. Jotiram, B.K. Palai, S. Bhattacharya, S. Aravinth, G. Gnanakumar, R. Subbiah, M. Chandrakasu, Investigating mechanical strength of a natural fibre polymer composite using SiO2 nano-filler, Mater. Today: Proc. 56 (2022) 1522–1526, https://doi.org/10.1016/j.matpr.2022.01.176.

[42] P. Madhu, M. Sanjay, P. Senthamaraikannan, S. Pradeep, S. Saravanakumar, B. Yogesha, A review on synthesis and characterization of commercially available natural fibers: Part II, J. Nat. Fibers 16 (2019) 25–36, https://doi.org/10.1080/15440478.2017.1379045.

[43] J. Ma, G. Yang, J. Mao, F. Xu, Characterization of anatomy, ultrastructure and lignin microdistribution in Forsythia suspensa, Ind. Crop. Prod. 33 (2011) 358–363, https://doi.org/10.1016/j.indcrop.2010.11.009.

[44] Q. Zhao, C. Qian, L. Harper, N. Warrior, Finite element study of the microdroplet test for interfacial shear strength: effects of geometric parameters for a carbon fibre/epoxy system, J. Compos. Mater. 52 (2018) 2163–2177, https://doi.org/10.1177/0021998317740943.

[45] F. Laifa, M. Rokbi, S. Amroune, M. Zaoui, Y. Seki, Investigation of mechanical, physicochemical, and thermal properties of new fiber from Silybum marianum bark fiber, J. Compos. Mater. 56 (2022) 2227–2238, https://doi.org/10.1177/00219983221090020.

[46] A. Balaji, K. Nagarajan, Characterization of alkali treated and untreated new cellulosic fiber from Saharan aloe vera cactus leaves, Carbohydrate Polymers 174 (2017) 200–208, https://doi.org/10.1016/j.carbpol.2017.06.065.

[47] J. Binoj, R.E. Raj, V. Sreenivasan, G.R. Thusnavis, Morphological, physical, mechanical, chemical and thermal characterization of sustainable Indian Areca fruit husk fibers (Areca Catechu L.) as potential alternate for hazardous synthetic fibers, Journal of Bionic Engineering 13 (2016) 156–165, https://doi.org/10.1016/S1672-6529(14)60170-0.

[48] P. Manimaran, S. Saravanan, M. Sanjay, S. Siengchin, M. Jawaid, A. Khan, Characterization of new cellulosic fiber: Dracaena reflexa as a reinforcement for polymer composite structures, J. Mater. Res. Technol. 8 (2019) 1952–1963, https://doi.org/10.1016/j.jmrt.2018.12.015.

[49] S. Indran, R.E. Raj, Characterization of new natural cellulosic fiber from Cissus quadrangularis stem, Carbohydrate polymers 117 (2015) 392–399, https://doi.org/10.1016/j.carbpol.2014.09.072.

[50] M. Sarikanat, Y. Seki, K. Sever, C. Durmuşkahya, Determination of properties of Althaea officinalis L.(Marshmallow) fibres as a potential plant fibre in polymeric composite materials, Compos. B Eng. 57 (2014) 180–186, https://doi.org/10.1016/j.compositesb.2013.09.041.

[51] P. Manimaran, V. Vignesh, A. Khan, G.P. Pillai, K. Nagarajan, M. Prithiviraj, A.N. Al-Romaizan, M.A. Hussein, M. Puttegowda, A.M. Asiri, Extraction and characterization of natural lignocellulosic fibres from Typha angustata grass, Int. J. Biol. Macromol. 222 (2022) 1840–1851, https://doi.org/10.1016/j.ijbiomac.2022.09.273.

[52] R. Dalmis, S. Köktaş, Y. Seki, A.Ç. Kılınç, Characterization of a new natural cellulose based fiber from Hierochloe Odarata, Cellulose 27 (2020) 127–139, https://doi.org/10.1007/s10570-019-02779-1.

[53] P. Manimaran, S. Saravanan, M. Sanjay, M. Jawaid, S. Siengchin, V. Fiore, New lignocellulosic aristida adscensionis fibers as novel reinforcement for composite materials: extraction, characterization and weibull distribution analysis, J. Polym. Environ. 28 (2020) 803–811, https://doi.org/10.1007/s10924-019-01640-7.

[54] A.B.A. Sukmana, I. Widyaningrum, R.K. Lani, S. Kasmiyati, Characterization of Ficus benjamina and Artocarpus heterophyllus proteases as potential rennet alternatives, Biosaintifika: Journal of Biology & Biology Education 12 (2020) 213–219, https://doi.org/10.15294/biosaintifka.v12i2.23516.

[55] P. Baskaran, M. Kathiresan, P. Senthamaraikannan, S. Saravanakumar, Characterization of new natural cellulosic fiber from the bark of dichrostachys cinerea, J. Nat. Fibers 15 (2018) 62–68, https://doi.org/10.1080/15440478.2017.1304314.

[56] M. Maheshwaran, N.R.J. Hyness, P. Senthamaraikannan, S. Saravanakumar, M. Sanjay, Characterization of natural cellulosic fiber from Epipremnum aureum stem, J. Nat. Fibers 15 (2018) 789–798, https://doi.org/10.1080/15440478.2017.1364205.

[57] M. Maran, R. Kumar, P. Senthamaraikannan, S. Saravanakumar, S. Nagarajan, M. Sanjay, S. Siengchin, Suitability evaluation of Sida mysorensis plant fiber as reinforcement in polymer composite, J. Nat. Fibers 19 (2022) 1659–1669, https://doi.org/10.1080/15440478.2020.1787920.

[58] N. Sakji, M. Jabli, F. Khoffi, N. Tka, R. Zouhaier, W. Ibala, H. Mohamed, B. Durand, Physico-chemical characteristics of a seed fiber arised from Pergularia Tomentosa L, Fibers Polym. 17 (2016) 2095–2104, https://doi.org/10.1007/s12221-016-6461-4.

[59] D. Ravindran, S.B. SR, S. Padma, S. Indran, D. Divya, Characterization of natural cellulosic fiber extracted from Grewia damine flowering plant's stem, Int. J. Biol. Macromol. 164 (2020) 1246–1255, https://doi.org/10.1016/j.ijbiomac.2020.07.225.

[60] S. Amroune, A. Bezazi, A. Belaadi, C. Zhu, F. Scarpa, S. Rahatekar, A. Imad, Tensile mechanical properties and surface chemical sensitivity of technical fibres from date palm fruit branches (Phoenix dactylifera L.), Compos. Appl. Sci. Manuf. 71 (2015) 95–106, https://doi.org/10.1016/j.compositesa.2014.12.011.

[61] J. Ahmed, M. Balaji, S. Saravanakumar, P. Senthamaraikannan, A comprehensive physical, chemical and morphological characterization of novel cellulosic fiber extracted from the stem of Elettaria cardamomum plant, J. Nat. Fibers 18 (2021) 1460–1471, https://doi.org/10.1080/15440478.2019.1691121.

[62] N. Saravanan, P. Sampath, T. Sukantha, T. Natarajan, Extraction and characterization of new cellulose fiber from the agrowaste of lagenaria siceraria (bottle guard) plant, Journal of Advances in chemistry 12 (2016) 4382–4388, https://doi.org/10.24297/jac.v12i9.3991.

[63] R. Kumar, N.R.J. Hynes, P. Senthamaraikannan, S. Saravanakumar, M. Sanjay, Physicochemical and thermal properties of ceiba pentandra bark fiber, J. Nat. Fibers 15 (2018) 822–829, https://doi.org/10.1080/15440478.2017.1369208.

[64] Z. Belouadah, A. Ati, M. Rokbi, Characterization of new natural cellulosic fiber from Lygeum spartum L, Carbohydrate polymers 134 (2015) 429–437, https://doi.org/10.1016/j.carbpol.2015.08.024.

[65] V. Fiore, T. Scalici, A. Valenza, Characterization of a new natural fiber from Arundo donax L. as potential reinforcement of polymer composites, Carbohydrate polymers 106 (2014) 77–83, https://doi.org/10.1016/j.carbpol.2014.02.016.

[66] A. Jabbar, J. Militký, J. Wiener, M.U. Javaid, S. Rwawiire, Tensile, surface and thermal characterization of jute fibres after novel treatments, Indian J. Fiber Textil Res. 41 (2016) 249–254, https://doi.org/10.56042/ijftr.v41i3.7896.

[67] R. Kumar, A. Meena, A. Chopra, A. Kumar, Keratin gene expression differences in wool follicles and sequence diversity of high glycine-tyrosine keratin-associated proteins (kaps) in magra sheep of India, J. Nat. Fibers 17 (2018) 1257–1263, https://doi.org/10.1080/15440478.2018.1558157.

[68] T.A. Tamanna, S.A. Belal, M.A.H. Shibly, A.N. Khan, Characterization of a new natural fiber extracted from Corypha taliera fruit, Sci. Rep. 11 (2021) 7622, https://doi.org/10.1038/s41598-021-87128-8.

[69] M. Maache, A. Bezazi, S. Amroune, F. Scarpa, A. Dufresne, Characterization of a novel natural cellulosic fiber from Juncus effusus L, Carbohydrate polymers 171 (2017) 163–172, https://doi.org/10.1016/j.carbpol.2017.04.096.

[70] J.P.V. Diaz, F. de Andrade Silva, J.R.M. d'Almeida, Effect of peach palm fiber microstructure on its tensile behavior, Bioresources 11 (2016) 10140–10157, https://doi.org/10.15376/biores.11.4.10140-10157.

[71] P. Manimaran, P. Senthamaraikannan, M. Sanjay, M. Marichelvam, M. Jawaid, Study on characterization of Furcraea foetida new natural fiber as composite reinforcement for lightweight applications, Carbohydrate polymers 181 (2018) 650–658, https://doi.org/10.1016/j.carbpol.2017.11.099.